

Tracking of Special Objects with Parallel Manipulator using Inverse Kinematics Approach

Dev Kunwar Singh Chauhan^{1a}, Jishnu A.K.^{1b}, Himanshu Tandon^{1c}, Pandu R Vundavilli^{1d}

School of Mechanical Sciences, IIT Bhubaneswar, Bhubaneswar, Odisha-752050¹
dkc10@iitbbs.ac.in^a, jak10@iitbbs.ac.in^b, ht10@iitbbs.ac.in^c, pandu@iitbbs.ac.in^d

ABSTRACT

The parallel manipulator is a very precise and accurate mechanism over serial mechanism, which can withstand high payloads. It is used in a wide range of applications in the prominent areas, such as aircraft testing, flight simulator, 3D printing, and in medical applications. In the present paper, an attempt is made to track the special objects using a 6-DOF parallel manipulator after utilizing inverse kinematics. The manipulator used here is Physik Instrument (PI) based 6-DOF SPS HEXAPOD. This work is divided into two parts. First one is to find the position and orientation of 3D-object using two HD cameras mounted in two mutually perpendicular planes. The second task involves the execution of the actual motion of parallel manipulator joints derived using the concept of inverse kinematics approach for tracking of that object. Simulations are performed in MATLAB environment for the inverse kinematics of the Stewart-platform. The experimental results show that the Stewart parallel manipulator has successfully tracked the objects that are moving in straight and circular paths.

Keywords: Parallel manipulator; Stewart platform; inverse kinematics; object tracking.

1. INTRODUCTION

Recently researchers are giving more attention to parallel manipulators when compared with the serial manipulators because of their superior performance in terms of accuracy, rigidity and load-carrying capacity. Moreover, some of the manipulators are already well established in industries for various applications. Initially, Merlet and Bonev¹ introduced the parallel manipulator based on the drawbacks of the existing serial manipulators. The developed parallel manipulator was very accurate and precise when compared with the existing serial manipulators. In 1942 Willard² designed a new parallel manipulator which was used for automatic spray painting applications. In addition to the above work, in 1947 Enrich Gough³ developed a first well-known hexapod with six struts symmetrically forming an octahedron called Universal tire-testing machine to counter the aero-landing load problems. Later on, in 1965 the author⁴ designed a parallel-actuated mechanism as a 6-DOF which is known as Stewart platform. The developed model was different from the octahedral hexapod. In general parallel manipulator is multiple closed-loop kinematic structures but the serial manipulators are the open-chain kinematic structure. Due to the closed-loop kinematic structure, the parallel manipulators have a very high load to weight ratio than the serial one. Alongside, these manipulators have used for high powered machining applications like

punching related operation in automation along with light machining applications such as drilling, milling and finishing related operations. These manipulators have high stiffness and rigidity all over the work volume. Parallel manipulators are very pretty and straight forward⁵ to perform the inverse kinematics and there is no difficulty while obtaining the equations using the geometry of the manipulator. Moreover, the dynamic analysis⁶ of the parallel manipulator is very difficult when compared with the serial manipulator due to the presence of several kinematic chains, all coupled to the platform. Out of several dynamic modelling methods, most of the researchers had used Lagrange-Euler formulation because of the reason that it gives good orderly analytical results. In the present research, the work divided into two folds. Firstly, it involves the detection of the object in 3-dimensional space. Secondly, to move the manipulator's upper plate to make it follow the object initially and then track that object automatically in real-time.

2. FORMULATION AND METHODOLOGY

Figure 1 shows the schematic diagram of the 6-DOF SPS parallel manipulator used in the present study. It consists of six identical extensible limbs connect at one end by the moving platform at points B_i by spherical joints and other end on the fixed base at points A_i by spherical joints. Each limb consists of an upper and a lower member connected by a prismatic joint. The six prismatic joints are the input to the manipulator.

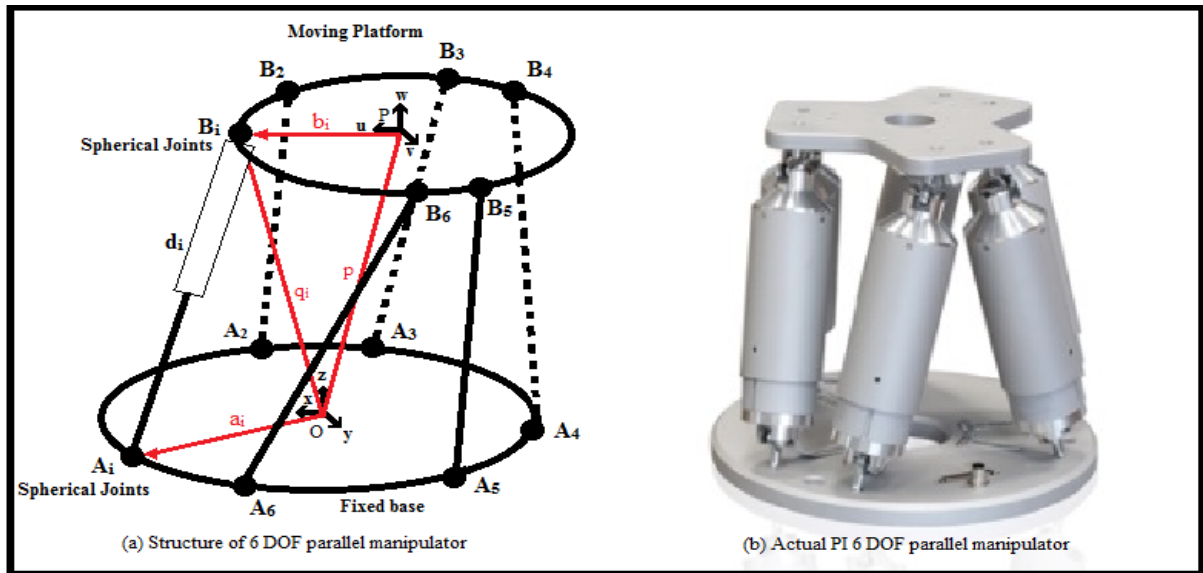


Figure 1. Schematic diagram 6 DOF parallel manipulator.

In the present research work, some assumptions are made and are as follows. For the analysis, the manipulator consists of two Cartesian coordinate systems namely (x-y-z) and (u-v-w). One attached to the fixed base at origin O and other at P to the moving platform, respectively.

The origin of frame O is the fixed base which is located at the centroid of the base and the origin P of the top moving plate is at the centroid of the top plate. The line joining the origin O and P is represented by a position vector p .

$$p = [p_x \quad p_y \quad p_z] \quad (1)$$

Moreover, the location of the moving platform can be described by a position vector, p and a rotation matrix, ${}^A_B R$. Let the rotation matrix be defined by the roll, pitch, and yaw angles as a rotation of ϕ_x about the fixed x - axis, a rotation of ϕ_y about the fixed y -axis, and a rotation of ϕ_z about the fixed y -axis. The rotation matrix ${}^A_B R$ obtained for the said transformations are given by using the following expression.

$${}^A_B R = \begin{bmatrix} [c(\phi_z) * c(\phi_y)] & [c(\phi_z) * s(\phi_y) * s(\phi_x) - s(\phi_z) * c(\phi_x)] & [c(\phi_z) * s(\phi_y) * c(\phi_x) + s(\phi_z) * s(\phi_x)] \\ [s(\phi_z) * s(\phi_y)] & [s(\phi_z) * s(\phi_y) * s(\phi_x) + c(\phi_z) * c(\phi_x)] & [s(\phi_z) * s(\phi_y) * c(\phi_x) - c(\phi_z) * s(\phi_x)] \\ [-s(\phi_y)] & [c(\phi_y) * s(\phi_x)] & [c(\phi_y) * c(\phi_x)] \end{bmatrix}$$

$s(\phi_i) = \sin(\phi_i)$ & $c(\phi_i) = \cos(\phi_i)$ Where $i = x, y, z$

The final transformation matrix (T) can be written as follows:

$$T = \begin{bmatrix} [c(\phi_y) * c(\phi_z)] & [-c(\phi_y) * s(\phi_z)] & [s(\phi_y)] & [p_x] \\ [s(\phi_x) * s(\phi_y) * c(\phi_z) + c(\phi_x) * s(\phi_z)] & [s(\phi_x) * s(\phi_y) * s(\phi_z) + c(\phi_x) * c(\phi_z)] & [c(\phi_y) * c(\phi_z)] & [p_y] \\ [-c(\phi_x) * s(\phi_y) * c(\phi_z) + s(\phi_x) * s(\phi_z)] & [c(\phi_x) * s(\phi_y) * s(\phi_z) + s(\phi_x) * c(\phi_z)] & [c(\phi_y) * s(\phi_z)] & [p_z] \\ [0] & [0] & [0] & [1] \end{bmatrix} \quad (2)$$

2.1 Position analysis

On referring to Fig. 1, the vector loop closure equation for each limb can be written as follows:

$$q_i = p + {}^A_B R \times b_i \quad (3)$$

$$q_i = a_i + d_i \quad (4)$$

where, $a_i = [a_{ix} \quad a_{iy} \quad a_{iz}]^T$ and $b_i = [b_{iu} \quad b_{iv} \quad b_{iw}]^T$ being the position vectors of a point A_i on the fixed frame of another point B_i on the moving frame respectively. Where, q_i is the position vector of B_i with respect to fixed coordinate system.

To be able to calculate the length d_i of i_{th} limb, the dot product of $a_i b_i$ is taken with itself. After doing that operation, one can obtain:

$$d_i^2 = [q_i - a_i]^T [q_i - a_i] \quad (5)$$

$i = 1, 2, \dots, 6$

After substituting the equation (4) in equation (5), the expanded form of expression is given as follows:

$$d_i^2 = [p + {}^A_B R \times b_i]^T [p + {}^A_B R \times b_i]$$

$$d_i^2 = p^T p + b_i^T b_i + a_i^T a_i + 2p^T [{}^A_B R b_i] - p^T a_i + 2[{}^A_B R b_i]^T a_i \quad (6)$$

The angle of the legs with the fixed base can be found as:

$$\theta_i = \tan^{-1} |d_i|/|a_i| \quad (7)$$

Finally, the structural animation of the kinematics of the manipulator is created using MATLAB as shown in Fig. 2, which shows that the default value of the position and orientation of the kinematic structure at X=0, Y=0, Z=200 mm, Yaw=0°, Pitch=0° and Roll=0°.

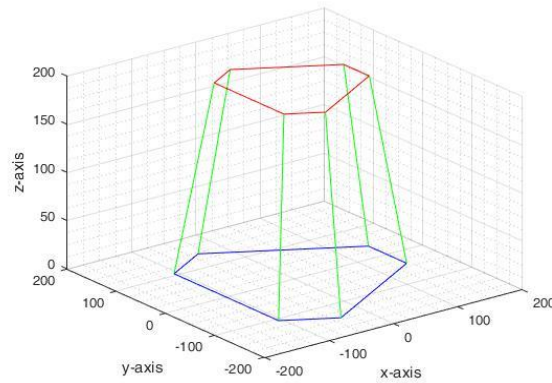


Figure 2. Kinematic structure.

2.2 Jacobian

It is the study that represents the relationship between the linear and angular velocity of a parallel manipulator. It reveals the relation between the joint velocity variables of the parallel manipulator to the moving platform. Let q be the joint variable and x be the location of the moving platform. Then the characteristic equation is given by:

$$f(X, q) = 0 \quad (8)$$

On differentiating the above equation, the relationship b/w the input joint rates and the end effector output velocity can be determined and is as follows.

$$J_x \dot{X} = J_q \dot{q}$$

Where,

$$J_x = \frac{\delta f}{\delta x}, J_q = \frac{\delta f}{\delta q}$$

Hence, the overall Jacobian is

$$\dot{q} = J\dot{X} \quad (9)$$

Where,

$$J = J_q^{-1} J_x$$

And \dot{q} is an m-dimensional vector that represents a set of actuated joint rates, \dot{X} is an n-dimensional output velocity vector of the end-effector, and J is the (n × m) Jacobian matrix.

2.3 Singularity conditions

Due to the existence of two Jacobian matrices, a parallel manipulator is said to be at singular configuration when either J_x or J_q or both are singular⁷. Three different types of singularities can be identified. The first one is related to the inverse kinematic singularities ($\det(J_q) = 0$), second is direct kinematic singularities ($\det(J_x) = 0$), and third the one is a combination of both the said singularities ($\det(J_x) = 0$ and $\det(J_q) = 0$).

2.4 Manipulator dynamics

Once the kinematics has been derived, the dynamics of the whole system is calculated which is helpful to determine the kinetic energy required to move the platform. The kinetic and potential energy for both the legs and the platform is determined by using the following mathematical relation.

$$K = K(q, \dot{q}) = \frac{1}{2} \dot{q}^T M(q) \dot{q} \quad \text{Where } q \in R^n \text{ and } \dot{q} \in R^{n \times n} \quad (10)$$

$$P = P(q) \quad \text{Where } P(q) \in R^n \quad (11)$$

The kinetic energy of the moving platform is given as:

$$K_{up} = K_{up(trans)} + K_{up(rot)} \quad (12)$$

Where, $K_{up(trans)}$ is translate the kinetic energy of moving plate and $K_{up(rot)}$ is rotational kinetic energy of moving plate. The potential energy of moving platform is given as:

$$P_{up} = m_{up} g P_z X_p \quad (13)$$

Where, m_{up} is mass of upper moving plate of the Stewart platform.

It requires a precise strategy to calculate the kinetic and potential energy of the legs of the manipulator as shown in Ref. 6. It can be considered that a separate mass element with their own inertia as piston and cylinder are considered as linear actuators for the calculation of kinetic and potential energies of the legs, but it has difficulties in computer computations. Instead of using the former strategy, an attempt is made to treat them as a point mass for both the elements for calculation of kinetic and potential energies. This strategy gives more ease in computer computation. Mostashiri⁸ solved the manipulator dynamics by using both the strategies accurately and found approximately similar results and suggested to use later one instead of former to reduce the computation complexity. Thus, the dynamic equations are derived using Lagrange formulation:

$$\frac{d}{dt} \frac{\delta K(q, \dot{q})}{\delta \dot{q}} - \frac{\delta K(q, \dot{q})}{\delta q} + \frac{\delta P(q)}{\delta q} = \tau \quad (14)$$

3. SIMULATION AND EXPERIMENTAL WORK

The idea of simulation comes to mind because of the visualization, it provides about the motion and the work volume it covers. Simulation has been carried out in MATLAB, in which code for the Inverse Kinematic (IK) of a generic 6-DOF Stewart platform has been prepared. As the kinematic analysis is independent of the inertia of the platform and only depends upon the joint parameters, it can be simulated in MATLAB for its various parameters mainly the link

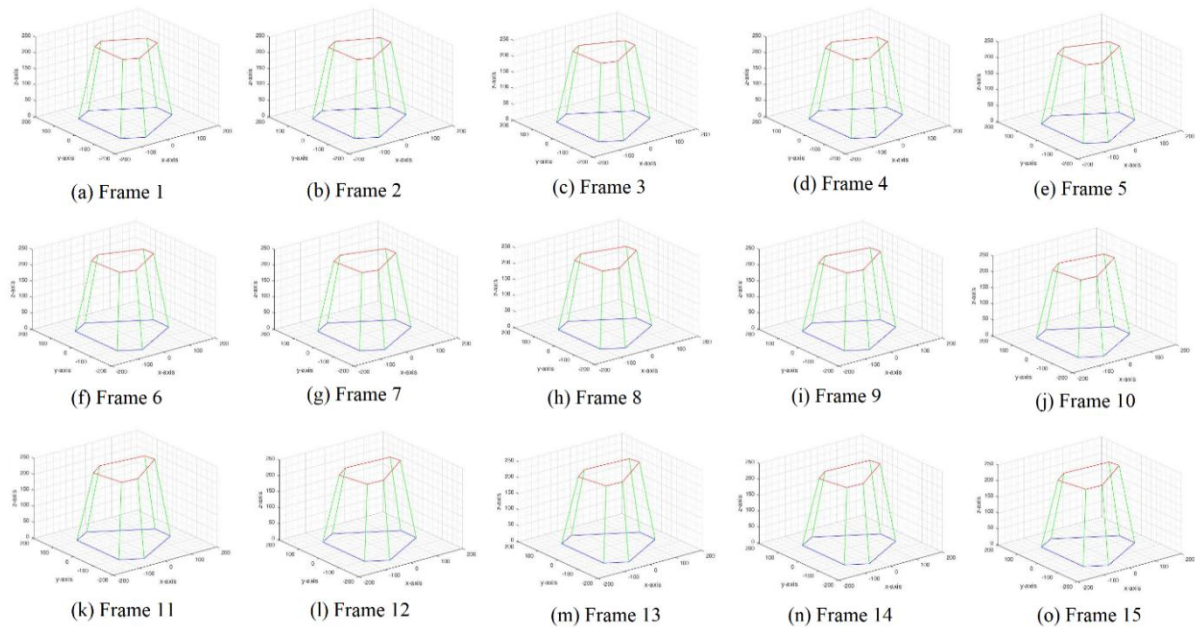


Figure 3. Time-scale for various position and orientations during simulation

lengths, and position analysis of various joints. Through simulations, one can find that the link parameters and the whole analysis of manipulator that how the platform will move in actual practice. It is visualized very closely. The time-scale for various position and orientations during simulation are shown in Fig. 3. The various frames grabbed during the simulation are presented in Fig. 3.

Apart from this, experimental work has also been carried out in a real-time environment using

two cameras placed at the right angle to get the three-dimensional map of the target object. Also, it is used to detect the motion of the manipulator along with the object.



Figure 4. Experimental Setup.

The experimental setup is shown in Fig. 4. A red colour marking of plastic material over the moving platform at the centre is used to identify the centre of the platform. It is a kind of markings for detection purpose which forms a small but key part of the setup. There is a green colour laser specified as “Emob Green Laser 5Mw Pointer Pen” is also attached at the centre of the moving platform via acrylic sheet to detect the position and orientation of the platform. An electrical circuit is prepared and fixed on the top of the platform at a certain height. It includes white-coloured bulbs that glow in red. A total of 5 number of bulbs are fixed to the plate so that they can form straight and circular patterns.

A MATLAB code has been written to detect the object. The detection of the object is based on the colour recognition process that is R-G-B colour segregation; particularly the red colour has been chosen to be the detection colour of the object. Cameras are used to take snapshots of the object and the manipulator as a unit, the MATLAB code is used to detect the red colour only, and hence the object is detected. To move the hexapod in order to follow the

object another MATLAB code has been written in place of PI user interface. Three real time experiments have been performed and depicted in Fig. 5.

The first experiment is related to the detection and tracking of a stationary object. In the second experiment, an attempt is made to track the object moving in the 3-D space, in a straight-line manner. The third experiment is related to the real-time tracking of an object moving in a circular path. Various plots have been obtained showing the precision of positioning, velocities, motor power of the various links, which are given in the results and discussion section.

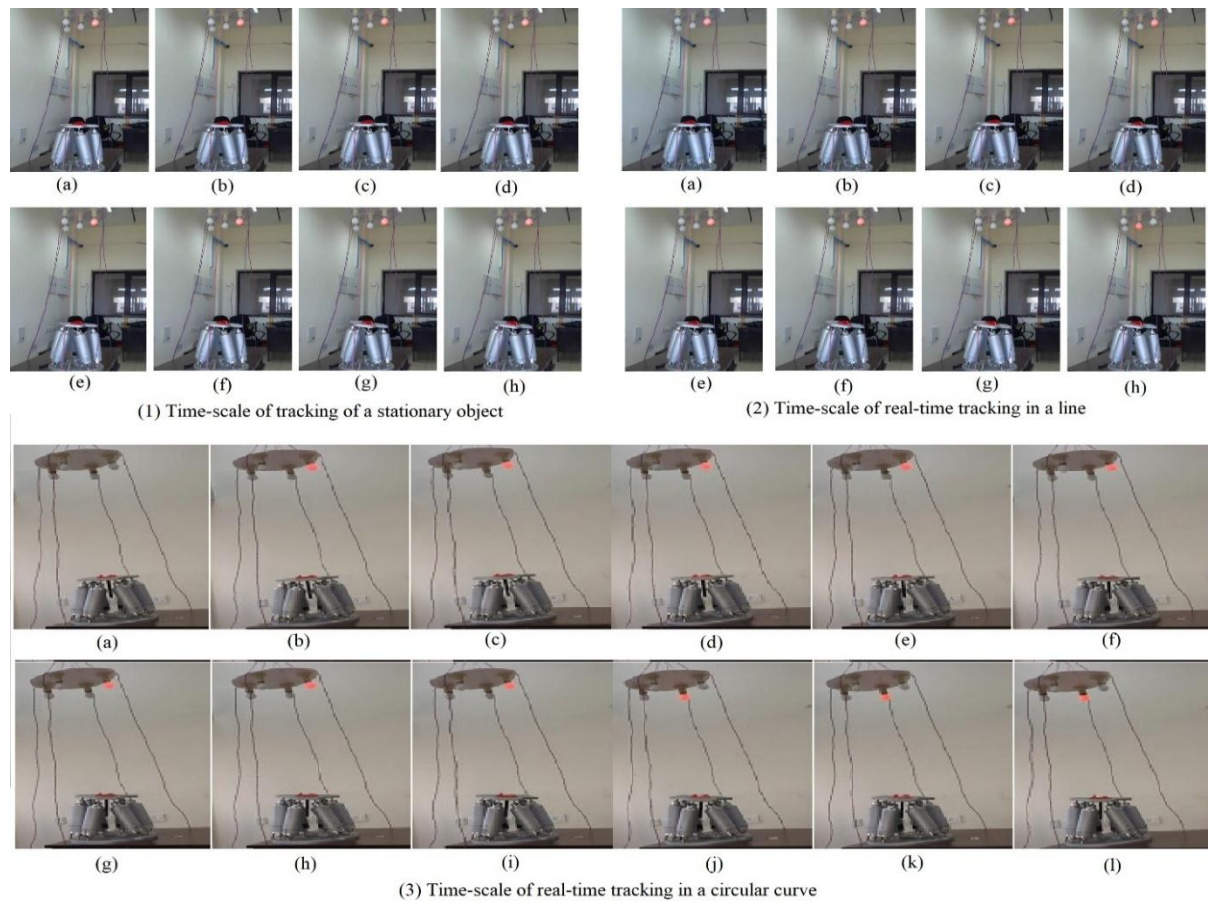


Figure 5. Depiction of step-by-step motion of the platform in real-time object tracking.

4. RESULTS AND DISCUSSION

4.1 Angular variation

While conducting the experiments for the case of the stationary object, the movement of the top platform can be controlled and can be made to move in a predefined manner. One such case is shown in Fig. 6. In this case, the top platform is allowed to move after following a fifth-order polynomial.

During the experiment, the data obtained from the two cameras are used to determine the position and orientation of the object to be tracked. Then the inverse kinematics approach is used to obtain the orientation of various joints involved in the movement. The information obtained various instances of time is used to establish the fifth-order polynomial that is used to move the platform. Figure 6 represents the plots of the angular displacement during the process of tracking the stationary object. The plots u and v represent the angular displacement about x- and y-axis, respectively.

4.2 Position variation

Figure 7 show the variation of the link lengths for the first, second, fifth and sixth links. One thing

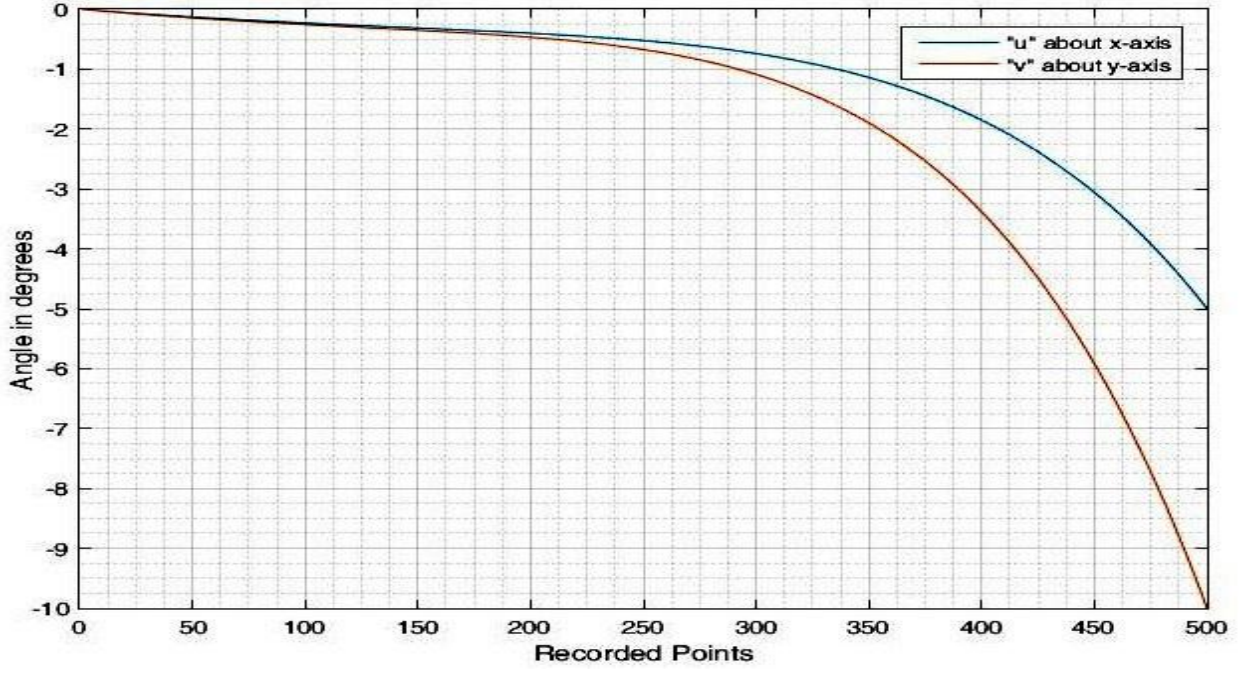


Figure 6. Angular variation.

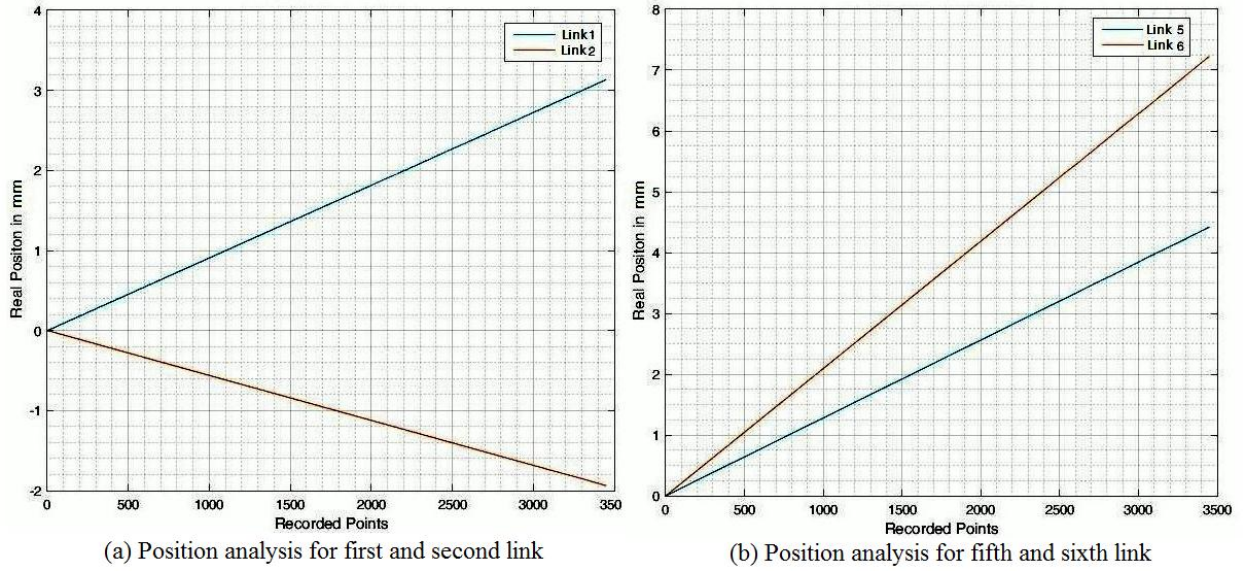


Figure 7. Position analysis.

to be noted that it (the plot) start with the zero value, it is because during the motion all the links are of equal lengths. From Fig. 7(a), the variation in the length of the strut is up to 3.1341 mm for the first link and -1.9377 mm for the second link. Thus their actual length is 209.1431 mm and 204.0623 mm respectively.

4.3 Velocity variation

Figure 8 shows the variation of the velocities for the links 1, 2, 5 and 6 during the motion of the hexapod. These are obtained directly from the controller which is made to move the

manipulator in a defined way using the inverse kinematic approach. The variations are shown in Fig. 8(a) and 8(b) are plotted with respect to the recorded (step) points.

From the plots, for link 1 & 2, it is seen that the velocity for the link 2 is varying in the negative sense. The reason for the negative value is due to the contraction of the link 2 during the motion of the platform. The other links velocities vary as usual like the min value for the link 1 is -1.5244 mm/sec and its max value are -0.5081 mm/sec.

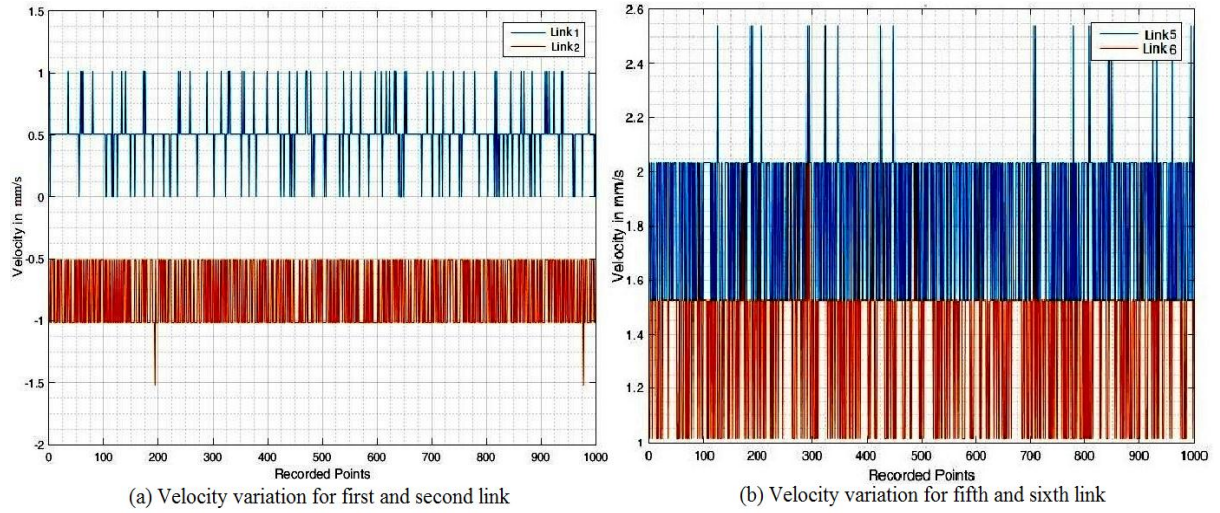


Figure 8. Velocity variations of links.

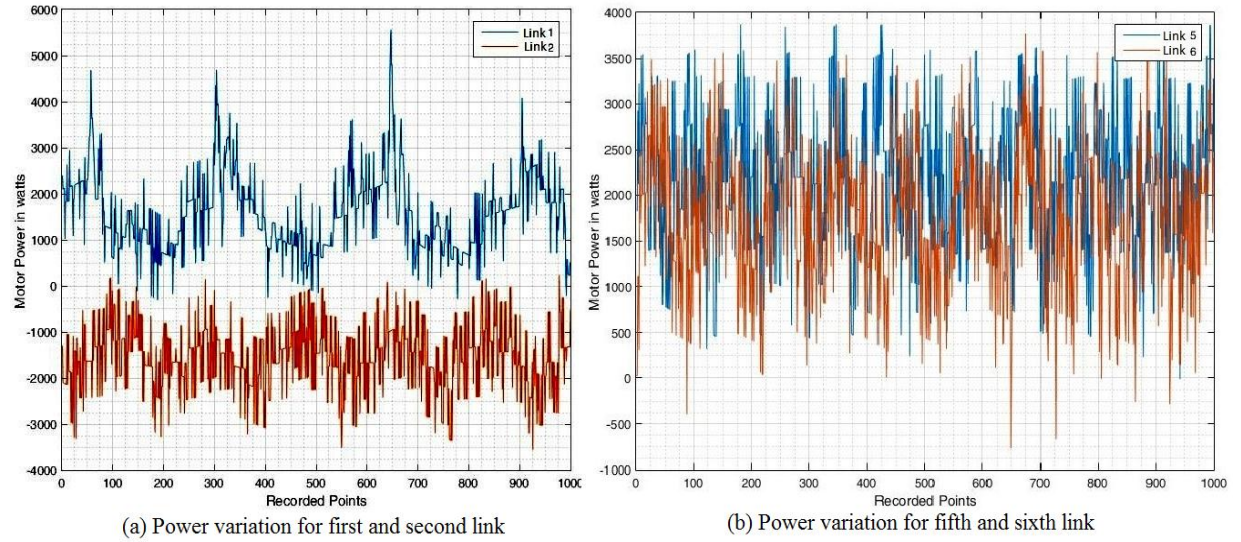


Figure 9. Power variations of links.

4.4 Power variation

Figure 9 shows the variation in power requirement for the links during operation. From Fig. 9(a) the graph for link 2 is always on the negative side. This only shows the reversal in the direction of the link, because the link is contracted to accommodate the motion of the platform. The plot for link 1 and 2, and links 5 and 6 is normal as shown in Fig. 9 (a) and

9(b). The maximum and minimum value of power in case of link 2 is 234 watts and -3561 watts respectively. The maximum value for power in case of links 1, 5 and 6 are seen to be equal to 5561 w, 3869 w, and 3778 w, respectively.

5. CONCLUSIONS

After examining various strengths and limitations of the 6-DOF parallel manipulator, a specific application of spatial object tracking is attempted. Using Inverse-Kinematics approach (IKA) a methodology for tracking of the spatial object is formulated. MATLAB is used as the computational tool for using the Inverse-Kinematics approach (IKA). The results obtained from the simulation are tested in a real-world application, by fabricating a setup which would generate three different configurations of spatial object motion. Various plots for determining link lengths, velocities and generated torques are obtained from the data acquired from the experimentation. The data acquired gave a fair idea of the motion generated by the manipulators, and its power consumption.

REFERENCES

1. Bonev I. "The true origins of parallel robots". *ParalleMIC Rev.*, vol. no. 1, pp. 1-6, 2003.
2. Pollard. "WLV. Position Controlling Apparatus". *US Pat No 2,286,571*, 1942.
3. Gough VE. "Universal tyre test machine". *Proc FISITA 9th Int Tech Congr, London*, pp. 117-137, 1962.
4. Stewart D. "A Platform with Six Degrees of Freedom". *Proc Inst Mech Eng.*, 180(1), pp. 371-386, 1965.
5. Dasgupta B, Mruthyunjaya TS. "Stewart platform manipulator: A review". *Mech Mach Theory*, **35**(1), pp. 15-40, 2000.
6. Lebret G, Liu K, Lewis FL. "Dynamic analysis and control of a stewart platform manipulator". *J Robot Syst.* **10**(5), pp. 629-655, 1993.
7. Liu K, Lewis F, Lebret G, Taylor D. "The singularities and dynamics of a Stewart platform manipulator". *J Intell Robot Syst.* **8**(3), pp. 287-308, 1993.
8. Mostashiri N, Akbarzadeh A, Dhupia J, Verl A, Xu W. "A Comprehensive Inverse Dynamics Problem of a Stewart Platform by Means of Lagrangian Formulation". 11-October-2017.